**WATER STORAGE CAPACITY OF THE MARTIAN MANTLE THROUGH TIME.** J. Dong[1*], R. A. Fischer[1], L. P. Stixrude[2], C. R. Lithgow-Bertelloni[2], Z. T. Eriksen[1] and M. C. Brennan[1], [1]Department of Earth and Planetary Sciences, Harvard University, Cambridge, Massachusetts 02138, USA. [2]Department of Earth, Planetary, and Space Sciences, University of California, Los Angeles, California 90095, USA. [*]Correspondence to: Junjie Dong (junjiedong@g.harvard.edu)

**Introduction:** Water has likely been stored in the Martian mantle, primarily in nominally anhydrous minerals (NAMs). The short-lived early hydrosphere and intermittently flowing water on the Martian surface may have been supplied and replenished by magmatic degassing of water from the mantle. Estimating the water storage capacity of the solid Martian mantle places important constraints on its water inventory and helps elucidate the sources, sinks, and temporal variations of water on Mars. In this study, we applied a bootstrap aggregation method to investigate the effects of iron on water storage capacities in olivine (*ol*), wadsleyite (*wd*), and ringwoodite (*rw*), based on high-pressure experimental data compiled from the literature, and we provided a quantitative estimate of the upper bound of the bulk water storage capacity in the FeO-rich solid Martian mantle.

**Equilibrium Phase Assemblages of Martian Mantle Rocks**: We computed a series of adiabatic temperature gradients ("aerotherms") of a simplified Martian mantle composition as a function of pressure for potential temperatures ($T_p$) from 1500 K to 1900 K, using the thermodynamic code HeFESTo and the self-consistent parameter set contained therein [1]. The simplified bulk composition of the Martian mantle in our model was a six-component system of $Na_2O$–CaO–FeO–MgO–$Al_2O_3$–$SiO_2$, with abundances based on Taylor (2013) [2].

**$H_2O$ Storage Capacities of Martian Mantle NAMs**: In calculating the water storage capacity of Martian mantle rocks, the water storage capacities of individual NAMs at each pressure and temperature were estimated and summed. The water storage capacities of the major NAMs in the Martian mantle assemblages (*ol*, *wd*, and *rw*) can be parameterized as (see more details in Dong et al., 2021 [3]):

$$\ln\left(c_{H_2O}\right) = a + \frac{n}{2} \cdot \ln f_{H_2O}(P, T) + \frac{b + c \cdot P + d \cdot X_{Fe}}{T} \quad (1)$$

with $T$ in kelvin (K), $P$ in gigapascals (GPa), $f_{H_2O}$ (water fugacity) in GPa, and $X_{Fe}$ (iron content) in mole fraction. The constants $a$, $b$, and $c$ are related to the changes in entropy, enthalpy, and volume of the hydration reaction, respectively; $d$ expresses the effect of iron (as FeO); and $n$ is the fugacity exponent.

To fit Equation 1 for each NAM, we used an updated version of a compilation data set of experimentally determined water storage capacities (in *ol*, *wd*, and *rw*) based on Dong et al. (2021) [3].

The water storage capacity in bulk Martian mantle rocks, $c_{H_2O}^{\text{mantle rock}}$, can then be calculated by averaging the water storage capacities of the major NAM phases at each $P$–$T$ (i.e., olivine or its polymorphs (i) and other coexisting minerals (j)):

$$c_{H_2O}^{\text{mantle rock}} = \left(c_{H_2O}^{\text{NAM}}\right)_i \cdot \left(X_i + \sum_j \left(X_j \cdot D_{H_2O}^{i/j}\right)\right) \quad (2)$$

where $D_{H_2O}^{i/j}$ is the water partition coefficient between i and j, $\left(c_{H_2O}^{\text{NAM}}\right)_i$ is the water storage capacity of olivine or its polymorphs, and $\left(c_{H_2O}^{\text{NAM}}\right)_j = \left(c_{H_2O}^{\text{NAM}}\right)_i \cdot D_{H_2O}^{i/j}(T, P, X_{Al})$ is the water storage capacity of coexisting mantle minerals. Details of the parameterizations for these partition coefficients as a function of temperature, pressure, and aluminum content, $X_{Al}$, can be found in Dong et al. (2021) [3].

**The Effect of Iron on the Bulk Martian Mantle $H_2O$ Storage Capacity:** Previous experiments demonstrated that the water storage capacity of *ol* increases by a factor of ~2–3 as its $X_{Fe}$ is increased from 0.2 to 0.4 at 3–6 GPa [4], so at least for olivine, iron has noticeable effects on water storage capacity at $X_{Fe} > 0.2$. However, no experimental study has systematically investigated the effects of iron on the water storage capacities of *wd* and *rw* with $X_{Fe} > 0.2$. If we directly fit Equation 1 to the compiled experimental dataset with the $\frac{d \cdot X_{Fe}}{T}$ term, the scarcity and imbalance of iron-rich samples, in particular for *wd* and *rw*, may cause an overfitting of $d$. To minimize overfitting $d$, while also incorporating all experimental measurements into our estimate of the Martian bulk mantle water storage capacity and its uncertainty, we applied a statistical method called "bootstrap aggregation" or "bagging". We first resampled the literature data with replacement and created $10^4$ copies of the bootstrapped dataset. We then fit a separate set of water storage capacity models (for each of *ol*, *wd*, and *rw*; Equation 1) to each resampled copy of the dataset, resulting in $10^4$ mantle water storage capacity profiles along each adiabat. Finally, we aggregated the $10^4$ water storage capacity

profiles as a function of depth for each $T_p$ and obtained the best-fit profiles by model averaging (mean).

**Depth-Dependent Profiles of $H_2O$ Storage Capacity in Martian Mantle Rocks**: We found that the maximum water storage capacity along Martian adiabats is often reached in *wd* within the *ol–wd* transition region (0.5–1.3 wt%, Fig. 1a–c), where the lower temperatures and higher $X_{Fe}$ in *wd* give rise to a higher water storage capacity (iron preferentially partitions into *wd* within the *ol–wd* transition region). Other abrupt changes in the profiles are consequences of phase transformations in the Martian mantle. The relatively large uncertainties in the extrapolation of the iron effect on the *wd* water storage capacity are manifested in the increased variations in the water storage capacity profiles of the deeper Martian mantle (*wd*-dominated layers) in Fig. 1a–c.

**Estimates of the Solid Martian Mantle $H_2O$ Storage Capacity as a Function of Mantle $T_p$:** The total water storage capacity integrated over depth for the solid Martian mantle was calculated for each $T_p$ from 1500 K to 1900 K (Fig. 1d–e). For the present-day Martian mantle with $T_p$ = 1600 K, the bulk mantle water storage capacity is $9.0^{+2.8}_{-2.2}$ km global equivalent layer (GEL). If the Martian mantle was 200 K hotter at the beginning of the Noachian (~4.1 Ga [5]), its mantle water storage capacity would have been $6.1^{+1.9}_{-1.7}$ km GEL for $T_p$ =1800 K. These water storage capacities for the early Noachian ($T_p$ = 1800 K) are ~2.9 km GEL smaller than the present-day water storage capacity ($T_p$ = 1600 K).

**Comparing the Solid Mantle $H_2O$ Storage Capacities of Mars and Earth and Their Evolution Through Time:** The bulk water storage capacity of the Earth's mantle (~2.3 OM, where OM is the modern surface ocean mass on Earth, ~1.335 × $10^{21}$ kg $H_2O$) is only a factor of ~2.3 larger than that of Mars (~1.0 OM) at $T_p$ = 1600 K, despite the volume of Earth's mantle (~9.1×$10^{11}$ $km^3$) being nearly 6.5 times larger than that of Mars (~1.4×$10^{11}$ $km^3$). This difference arises primarily from the Fe enrichment in the Martian mantle. Though the evolution of mantle water storage capacities in Earth and Mars follows the same increasing trend with secular cooling (Fig. 1e), mantle rehydration by subduction (e.g., [6]) may have been increasing Earth's actual mantle water content since the onset of plate tectonics (light blue dashed arrow in Fig. 1e). In contrast, Mars lacks efficient water recycling mechanisms (such as long-term subduction-driven plate tectonics [7]), so its actual mantle water content may have remained relatively low to the present (light red dashed arrow in Fig. 1e).

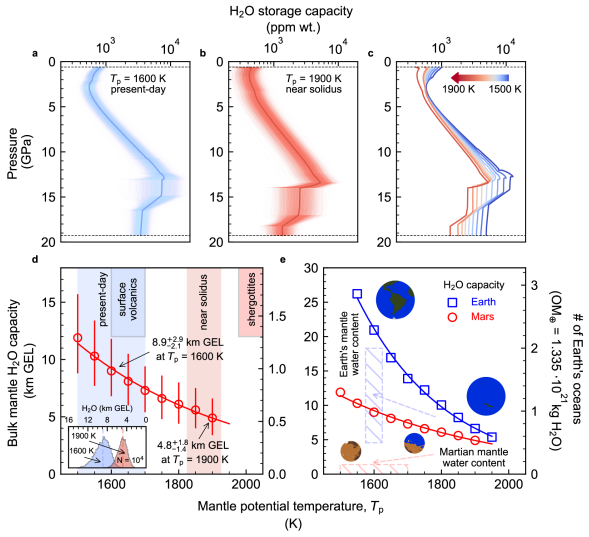


**Figure 1:** Water storage capacity of the solid Martian mantle. In the upper panels, the bold lines are the best-fit water storage capacity profiles along mantle adiabats at (a) $T_p$ = 1600 K, (b) $T_p$ = 1900 K, and (c) $T_p$ = 1500–1900 K, in increments of 50 K. The light curves in a and b are $10^4$ profiles from a representative set of "bagging" sampling. In the lower panels, the red open circles are the bulk water storage capacities for the solid Martian mantle at each $T_p$, which were calculated as the medians of $10^4$ "bagging" samples; the blue open squares are the bulk water storage capacities for the solid Earth's mantle estimated by Dong et al. (2021) [3]. In (d), the error bars represent the 5th and 95th percentiles of each distribution; the shaded areas are the estimated ranges for the Martian mantle $T_p$; and the boxes are the $T_p$ ranges estimated for different Martian basalt suites [5]. In the inset of (d), two distributions of "bagging" samples are shown, for $T_p$ = 1600 K (blue) and $T_p$ = 1900 K (red). The vertical dashed lines are the best-fit (model average or mean) bulk water storage capacity for each $T_p$. In (e), the hatched regions correspond to geochemical estimates of the actual mantle water contents of Mars and Earth.

**References:**

[1] Stixrude, L. and Lithgow-Bertelloni, C. (2011) *Geophys. J. Int.*, *184*(3), 1180–1213 [2] Taylor, G.J. (2013) *Chem. Erde*, *73*(4), 401–420 [3] Dong, J., et al. (2021) *AGU Adv.*, *2*(1), e2020AV000323. [4] Withers, A.C., et al. (2011) *Am. Mineral.*, *96*(7), 1039–1053. [5] Filiberto, J. (2017) *Chem. Geol.*, *466*, 1–14. [6] van Keken, P.E., et al. (2011) *J. Geophys. Res. Solid Earth*, *116*(B1). [7] Nimmo, F. and Tanaka, K. (2005) *Annu. Rev. Earth Planet. Sci.*, *33*, 133–161.